**Methane-Consuming Archaea Revealed by Directly Coupled Isotopic and Phylogenetic Analysis**

Victoria J. Orphan, *et al.*
*Science* **293**, 484 (2001);
DOI: 10.1126/science.1061338

7. X. Su, L. A. Kirkman, H. Fujioka, T. E. Wellems, *Cell* **91**, 593 (1997).
8. D. A. Fidock *et al.*, *Mol. Cell* **6**, 861 (2000).
9. B. A. Biggs *et al.*, *Proc. Natl. Acad. Sci. U.S.A.* **88**, 9171 (1991).
10. D. J. Roberts *et al.*, *Nature* **357**, 689 (1992).
11. J. D. Smith *et al.*, *Cell* **82**, 101 (1995).
12. X. Z. Su *et al.*, *Cell* **82**, 89 (1995).
13. D. I. Baruch *et al.*, *Cell* **82**, 77 (1995).
14. S. M. Rich, M. C. Licht, R. R. Hudson, F. J. Ayala, *Proc. Natl. Acad. Sci. U.S.A.* **95**, 4425 (1998).
15. X. Su, T. E. Wellems, *Genomics* **33**, 430 (1996).
16. T. J. Anderson, X. Z. Su, M. Bockarie, M. Lagog, K. P. Day, *Parasitology* **119**, 113 (1999).
17. W.-H. Li, *Molecular Evolution* (Sinauer, Sunderland, MA, 1997).
18. T. Lehmann, C. R. Blackston, S. F. Parmley, J. S. Remington, J. P. Dubey, *J. Parasitol.* **86**, 960 (2000).
19. M. J. Gardner *et al.*, *Science* **282**, 1126 (1998).
20. S. Bowman *et al.*, *Nature* **400**, 532 (1999).
21. Supplementary Web material (Methods and Figures) is available on *Science* Online at www.sciencemag.org/cgi/content/full/293/5529/482/DC1.
22. X. Su *et al.*, *Science* **286**, 1351. (1999).
23. T. A. Kunkel, *J. Biol. Chem.* **261**, 13581 (1986).
24. S. M. Rich, R. R. Hudson, F. J. Ayala, *Proc. Natl. Acad. Sci. U.S.A.* **94**, 13040 (1997).
25. S. L. Salzberg, M. Pertea, A. L. Delcher, M. J. Gardner, H. Tettelin, *Genomics* **59**, 24 (1999).
26. A. A. Escalante, E. Barrio, F. J. Ayala, *Mol. Biol. Evol.* **12**, 616 (1995).
27. D. J. Conway *et al.*, *Mol. Biochem. Parasitol.* **111**, 163 (2000).
28. F. B. Livingstone, *Am. Anthropol.* **60**, 533 (1958).
29. S. Jarcho, *Bull. Hist. Med.* **37**, 1 (1964).
30. L. J. Bruce-Chwatt, *Bull. WHO* **32**, 363 (1965).
31. M. Coluzzi, *Parassitologia (Rome)* **41**, 277 (1999).
32. A. L. Hughes, *Mol. Biol. Evol.* **9**, 381. (1992).
33. S. M. Rich, F. J. Ayala, *Proc. Natl. Acad. Sci. U.S.A.* **97**, 6994 (2000).
34. T. F. McCutchan, A. P. Waters, *Immunol. Lett.* **25**, 23 (1990).
35. We thank J. Hume and G. Ramirez for maintaining the parasite cultures. Supported by funding from NIH, the Burroughs-Wellcome Fund, and the Wellcome Trust. K.M.N. was supported by the Research Council of Norway.

# Methane-Consuming Archaea Revealed by Directly Coupled Isotopic and Phylogenetic Analysis

**Victoria J. Orphan,**[1]***** **Christopher H. House,**[2]*****† **Kai-Uwe Hinrichs,**[3] **Kevin D. McKeegan,**[4] **Edward F. DeLong**[1]†

Microorganisms living in anoxic marine sediments consume more than 80% of the methane produced in the world's oceans. In addition to single-species aggregates, consortia of metabolically interdependent bacteria and archaea are found in methane-rich sediments. A combination of fluorescence in situ hybridization and secondary ion mass spectrometry shows that cells belonging to one specific archaeal group associated with the *Methanosarcinales* were all highly depleted in $^{13}C$ (to values of −96‰). This depletion indicates assimilation of isotopically light methane into specific archaeal cells. Additional microbial species apparently use other carbon sources, as indicated by significantly higher $^{13}C/^{12}C$ ratios in their cell carbon. Our results demonstrate the feasibility of simultaneous determination of the identity and the metabolic activity of naturally occurring microorganisms.

Microbes critically impact global geochemical cycles. Although the general ecological importance of microbial activity is well recognized, the identity and involvement of microbes in specific biogeochemical cycles are often poorly understood. For example, the anaerobic oxidation of methane (AOM) is a widespread and geochemically well documented process [e.g., (*1*)], yet very little is known about the physiology, biochemistry, and identity of the microbes involved. One reason for this is that often the ecologically relevant microorganisms are difficult to isolate in pure culture. Approaches that combine phylogenetic and stable isotope analyses have considerable potential for linking microbial diversity with in situ activity (*2–4*). Recent studies that combine phylogenetic surveys of ribosomal RNAs (rRNAs) with structural and stable isotopic analyses of lipids have revealed new information about methane-oxidizing microbes in anoxic marine sediments (*3*, *5*, *6*). However, the stable isotopic and phylogenetic methods used in these studies were uncoupled, so identification of the specific microbes mediating AOM is based mainly on indirect lines of evidence.

Here, we report a cultivation-independent study of marine microbial assemblages in anoxic methane-rich sediments that combined microbial cell identification using ribosomal RNA-targeted fluorescent in situ hybridization (FISH) (*7*) with secondary ion mass spectrometry (SIMS) (*8*). After rRNA-targeted probes were applied to identify microbial cells, the stable isotope composition of the identified cells was determined by using SIMS. Coupled FISH-SIMS provided a measure of the stable carbon isotope composition of individual phylogenetically identified cell aggregates. Uncultured, naturally occurring microbial cells that utilize methane as the source of cell carbon could therefore be identified unambiguously.

Previous studies suggested that cell aggregates of archaea belonging to the *Methanosarcinales* (ANME-2 group), surrounded by sulfate-reducing bacteria related to the *De-*

**Table 1.** Carbon isotopic compositions (versus PDB) and source assignments of selected extracted archaeal ether lipids and bacterial fatty acids (FAs). SRB, sulfate-reducing bacteria.

| Compound | Eel River Basin, 3 to 5 cm | | Santa Barbara hydrocarbon seep | |
|---|---|---|---|---|
| | $\delta^{13}C$ (‰) | Source assignment | $\delta^{13}C$ (‰) | Source assignment |
| Archaeol | −104.1 | ANME-2 | Traces/not analyzed | Archaea |
| *sn*-2-Hydroxyarchaeol | −107.6 | ANME-2 | Traces/not analyzed | Archaea |
| *n*-C$_{14:0}$ FA | −69.1 | SRB | −22.7 | Algae, bacteria |
| *i*-C$_{15:0}$ FA | −51.3 | SRB, other bacteria | −25.4 | Bacteria mainly |
| *ai*-C$_{15:0}$ FA | −51.9 | SRB, other bacteria | −19.0 | Bacteria mainly |
| *n*-C$_{16:1(\omega7)}$ FA* | −62.8 | SRB | −26.0 | Algae, bacteria |
| *n*-C$_{16:1(\omega5)}$ FA* | −76.1 | SRB | −21.2 | Algae, bacteria |
| *n*-C$_{16:0}$ FA | −44.1 | SRB, other bacteria, algae | −20.3 | Algae, bacteria |
| 10-Me-C$_{16:0}$ FA | −69.4 | SRB | Not present | — |

*Double-bond positions were determined from nearby samples with almost congruent fatty acid distributions (*24*) and refer only to the sample from the Eel River Basin.

[1]Monterey Bay Aquarium Research Institute, Moss Landing, CA 95039, USA. [2]Department of Geosciences, The Pennsylvania State University, University Park, PA 16802, USA. [3]Department of Geology and Geophysics, Woods Hole Oceanographic Institution, Woods Hole, MA 02543, USA. [4]Department of Earth and Space Sciences, University of California, Los Angeles, CA 90095, USA.

*These authors contributed equally to the work.
†To whom correspondence should be addressed. E-mail: chouse@geosc.psu.edu and delong@mbari.org

*sulfosarcina,* were involved in AOM (*5*, *6*). To test this hypothesis, microbial cell aggregates were recovered from marine sediments (intervals 3 to 5 cm deep) at methane seeps in the Eel River Basin, California (*9*). The sediments contained highly $^{13}$C-depleted archaeal and bacterial lipid biomarkers (*10*) (Table 1). By using FISH-SIMS, $\delta^{13}$C (*11*) was profiled from the periphery to the interior of separate cell aggregates (in approximately 0.75-μm increments) by repeated sputtering of the aggregate surface with a Cs$^+$ beam (*12–15*). These analyses revealed that cell aggregates binding a specific archaeal probe (ANME-2) in their inner core, and a bacterial *Desulfosarcina-Desulfococcus* (DSS) probe on their periphery, were composed of extremely depleted carbon with $\delta^{13}$C values as low as –96‰ (Figs. 1 and 2, A and B). These isotopic signatures are best explained by assimilation of carbon from a $^{13}$C-depleted source. The only plausible source with sufficiently $^{13}$C-depleted carbon is methane and, indeed, the $\delta^{13}$C values of methane obtained from adjacent seep sites in Eel River Basin range between –63 and –35‰ (*16*).

In addition to putative syntrophic ANME-2/DSS consortia, cell aggregates that contained the archaeal ANME-2 group, but not bacteria, were also occasionally observed (Fig. 2, C and D). Isotopic analysis of these monospecific ANME-2 aggregations also revealed extreme $^{13}$C-depletions, reaching $\delta^{13}$C values of –85‰, again indicating that the major portion of their biomass was derived from methane. That these $\delta^{13}$C values are lower than coexisting methane indicates significant isotopic fractionation of the assimilated carbon by the methane-oxidizing archaeal group, ANME-2 (Fig. 3). Although bacteria-free aggregations of the *Methanosarcinales*-related ANME-2 group in methane-rich marine sediments have not been previously reported (*5*, *6*), our observations indicate that this archaeal group

may sometimes exist independently of syntrophic partners.

In contrast to the archaeal-bacterial consortia, the carbon isotopic compositions of other microbial aggregates from the same Eel River Basin sample were about –20‰. This value is consistent with assimilation of organic carbon derived from photosynthetic primary productivity or from the fixation of $CO_2$ (Fig. 2D). For comparison, we analyzed sulfate-reducing bacterial aggregates originating from a shallow water hydrocarbon seep offshore Santa Barbara, California. Microscopic surveys using FISH of the hydrocarbon-impregnated sediment sample revealed abundant bacterial aggregates phylogenetically related to the *Desulfosarcina*, but no ANME-2 archaea. Ion microprobe analyses of *Desulfosarcina* aggregates displayed $\delta^{13}$C values similar to those of sedimentary organic carbon (*17*) and oils from the underlying Monterey Formation (Fig. 2, E and F). Carbon isotopic compositions from fatty acids extracted from the hydrocarbon seep sediment ranged from –26 to –19‰ (Table 1). No lipids with isotopic compositions indicative of microbial utilization of methane-derived carbon were detected (*18*). Moreover, the fatty acid distribution from the oil seep differed significantly from that of the Eel River Basin methane seep, suggesting that these

two sites harbored different bacterial communities. Both lipid and whole-cell isotopic data suggest that anaerobic oxidation of methane is not a significant biogeochemical pathway at this site.

The variation in $\delta^{13}$C values of aggregates containing the archaeal ANME-2 was greater than that of other cell aggregates. Significant isotopic variations were observed between individual ANME-2/DSS consortia, with archaeal-bacterial aggregates falling into two isotopically distinct groups (Fig. 3). For aggregates with relatively high $\delta^{13}$C values, methane was probably not the exclusive carbon source. Despite the large range in isotopic values, all the ANME-2/DSS consortia exhibit lower $\delta^{13}$C values than *Desulfosarcina* cell clusters and other cell aggregates, which are characterized by average $\delta^{13}$C values in the range –30 to –15‰ (Fig. 3).

To date, there have been no reported studies of single-cell isotopic variation for microbes, making interpretations of the variability we observe difficult. Preliminary SIMS data obtained for reference from pure cultures of cyanobacteria revealed substantial carbon isotopic variation (*Gloeothece* sp. 27152: mean $\delta^{13}$C = –17.1 ± 2.1‰, SD = 7.5; *n* = 13; and *Gloeocapsa* sp. 29159: mean $\delta^{13}$C = –24.3 ± 1.3‰, SD = 6.3; *n* = 23), reflect-
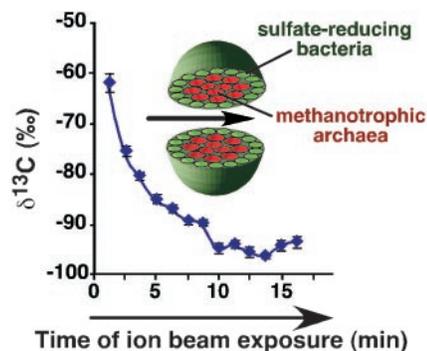
**Fig. 1.** A schematic diagram of an archaeal ANME-2/bacterial *Desulfosarcina* (DSS) aggregate, showing the direction of penetration of an ion beam, indicated by the arrow. The graph shows the $\delta^{13}$C profile obtained with the ion microprobe versus time (minutes of Cs$^+$ beam exposure) through the same 10-μm aggregate that is depicted in Fig. 2, A and B.

**Fig. 2.** Whole-cell FISH of methane-oxidizing consortia and other cell aggregates in methane seep sediments, identified microscopically and targeted with the ion microprobe. (**A**) Overlaid epifluorescent image of a Cy-3–labeled archaeal ANME-2 (in red) and fluorescein-labeled bacterial *Desulfosarcina* (DSS, in green) cell aggregate from Eel River Basin. (**B**) Corresponding DAPI (nonspecific stain for DNA) and average $\delta^{13}$C value of the aggregate obtained by SIMS. (**C**) Cy-3–labeled archaeal ANME-2 aggregate. (**D**) DAPI stain of same field showing isotopic values of both the ANME-2–targeted aggregate and a cell aggregate not targeted by either the archaeal ANME-2 or bacterial DSS rRNA probes. (**E**) Sulfate-reducing bacterial aggregates from a Santa Barbara hydrocarbon seep targeted with fluorescein-labeled bacterial DSS probe. (**F**) Corresponding DAPI stain of same field and average $\delta^{13}$C values obtained by SIMS. Scale bar, 10 μm in each panel.
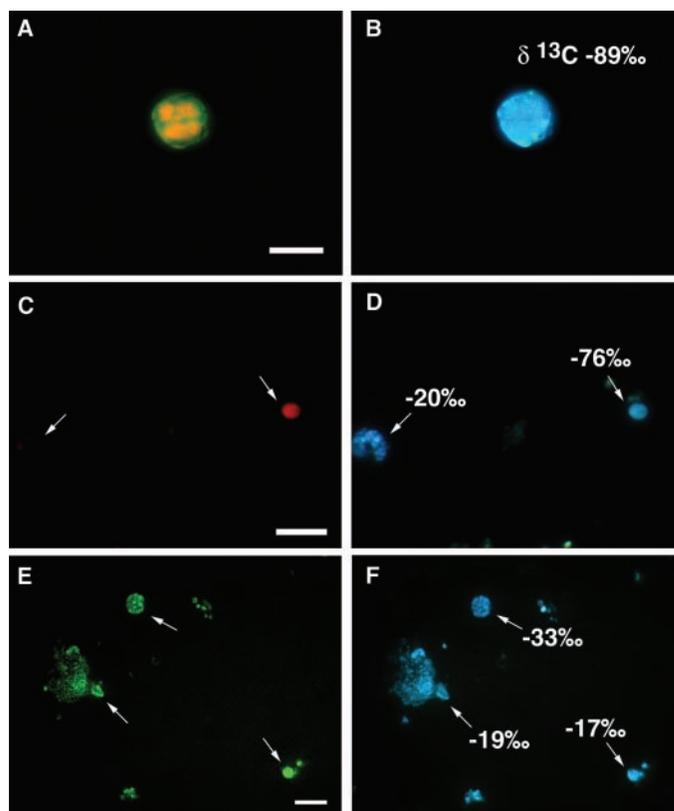
**Fig. 3.** Ion microprobe measured $\delta^{13}$C profiles for individual cell aggregates recovered from marine methane seep sediments (Eel River Basin[*] and Santa Barbara Basin) [12]. Numbers indicate sample number and designate the start of ion microprobe analysis for each cell aggregate. In most cases, extended analyses produced isotopically lighter values, as continued sputtering penetrated through the aggregate interior where the archaeal ANME-2 microbes are concentrated. In contrast, the bacterial samples (10 through 14) exhibited relatively constant $\delta^{13}$C profiles with depth. The hatched area represents the range of $\delta^{13}$C values measured for $CH_4$ extracted from pore water from adjacent Eel River Basin methane seeps (average −50‰; $n = 28$). The relatively high $\delta^{13}$C values for pore water $CH_4$ are likely due to isotopic enrichment from active methanotrophy.
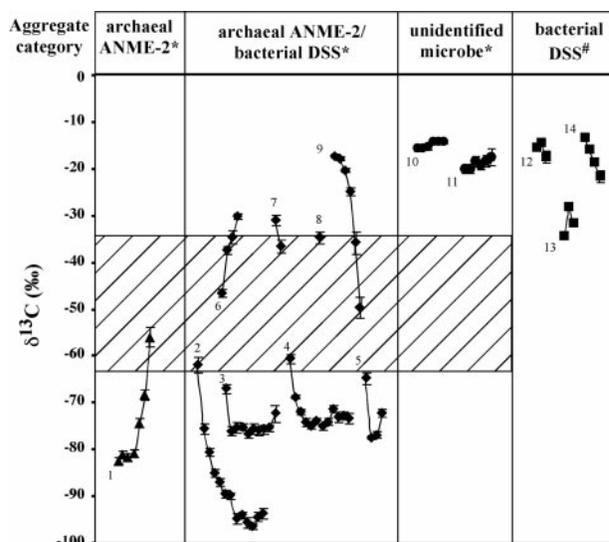
ing some degree of organism-specific heterogeneity probably magnified by closed-system culture conditions. Whatever the causes, the heterogeneity of isotopic values in cell populations does not appear to be an artifact of the SIMS procedure [19]. In the context of the cell aggregates analyzed, the large $\delta^{13}$C variations we observed may reflect differences in the relative proportion of bacterial and archaeal biomass; heterogeneity in physiological status; dilution of the isotopic signal by contaminating materials, such as sediment particles [20]; or isotope effects caused by methane depletion.

We also observed significant variation in $\delta^{13}$C between the outer and inner portions of some ANME-2/DSS cell clusters, which exhibit a distinctive isotopic trend to lower $\delta^{13}$C values with increasing penetration into the aggregate (Figs. 1 and 3). Notably, the average isotopic variation within single ANME-2/DSS aggregates was significantly greater (18‰; $n = 8$) than aggregates composed of other microbial species (5‰; $n = 5$). This observation suggests a highly $^{13}$C-depleted inner core of methane-oxidizing archaea, surrounded by a somewhat less $^{13}$C-depleted outer shell of sulfate-reducing bacteria. These cellular data are concordant with isotopic analyses of lipid biomarkers extracted from the same samples (Table 1). The somewhat lower (by about −10 to −20‰) $\delta^{13}$C values of the archaeal lipids compared with the total cell carbon determined by SIMS is in agreement with previous observations of isotopic compositions of individual lipids versus biomass of *Methanosarcina barkeri* grown on trimethylamine [21]. The isotope patterns we observed in the total carbon of individual ANME-2/DSS cell aggregates

are consistent with the transfer of methane-derived intermediates (possibly acetate or $CO_2$), in addition to hydrogen, from methane-consuming archaea to their sulfate-reducing bacterial partners [22, 23].

Although ion microprobe mass spectrometry has been used in diverse applications in the earth and planetary sciences, ranging from interplanetary dust particles [14] to microfossil analyses [13], this technique had not yet been applied to active microbial cells from environmental samples. The ability to microscopically characterize microbial cells directly with FISH-SIMS provides an effective strategy for identifying additional microbial groups participating in the anaerobic oxidation of methane, as chemotaxonomic and phylogenetic evidence indicates diverse microbial assemblages are involved in this process [6, 24–26]. This approach can provide direct information on the identity of environmentally relevant microorganisms, as well as their metabolic activities and ecological interactions, by using either naturally occurring or exogenously added stable isotopes as tracers.

**References and Notes:**
1. C. S. Martens, R. A. Berner, *Limnol. Oceanogr.* **22**, 10 (1977).
2. H. T. S. Boschker *et al.*, *Nature* **392**, 801 (1998).
3. K.-U. Hinrichs, J. M. Hayes, S. P. Sylva, P. G. Brewer, E. F. DeLong, *Nature* **398**, 802 (1999).
4. S. Radajewski, P. Ineson, N. R. Parekh, J. C. Murrell, *Nature* **403**, 646 (2000).
5. A. Boetius *et al.*, *Nature* **407**, 623 (2000).
6. V. J. Orphan *et al.*, *Appl. Environ. Microbiol.* **67**, 1922 (2001).
7. Whole-cell hybridization was performed as previously described [F.O. Glöckner, B. M. Fuchs, R. Amann, *Appl. Environ. Microbiol.* **65**, 3721 (1999) and (6)] by using the archaeal ANME-2 specific (EelMSMX932-cy3-AGCTCCACCCGTTGTAGT) and the bacterial *Desulfosarcina-Desulfococcus* (DSS658-fl-TCCACTTCCCTCTCCCAT) oligonucleotide probes (5). Hybridized cells were stained with a dilute 4′6′-diamidino-2-phenylindole (DAPI) so-

lution (5 μg/ml) for 1 min, washed, and examined dry under epifluorescence microscopy with an Axiophot 2 microscope by using a dry 80× objective (Leitz). Location of aggregates was recorded and documented for subsequent ion microprobe analyses with a series of phase contrast and epifluorescent images by using 10×, 40×, and 80× objectives. Aggregates were photographed by using a spot SP100 cooled digital color charge-coupled-device camera, and images of the dual-stained cell aggregates were overlaid in Adobe Photoshop 6.0. Because of the absence of mounting medium and the lower magnification and resolution of the dry 80× objective, the outlines of individual cells were not clearly resolved in the photographs. Hybridized slides were stored with a desiccant pack for up to 1 week at −20°C before ion microprobe analyses.
8. The University of California, Los Angeles, CAMECA ims 1270 ion microprobe was used to analyze the carbon isotopic composition of individual target cells and cells aggregates, deposited on the surface of clean glass slides, that were previously phylogenetically identified by FISH photomicroscopy. Secondary $C_2^-$ ions were sputtered by a 10- to 15-μm-diameter $Cs^+$ beam from the target biomass and analyzed by using a multicollector arrangement consisting of an electron multiplier on-axis (for detection of $^{12}$C/$^{13}$C$^-$) and a Faraday cup off-axis (for detection of $^{12}C_2^-$). Instrumental mass fractionation and relative detector efficiencies were calibrated by the analysis of graphite powder dried onto the surface of the glass slide. An appropriate correction was made to account for an observed ∼10.7‰ matrix effect between graphite and microbial cell biomass. The matrix effect between graphite and cell biomass was studied by comparing the mean observed $\delta^{13}$C value for cells of a particular laboratory cell culture to the bulk $\delta^{13}$C value of that culture determined by using conventional gas source mass spectrometry. The observed matrix effect between *Gloeothece* sp. 27152 cell biomass and graphite was 10.0 ± 2.2‰ ($n = 13$), between *Gloeocapsa* sp. 29159 cell biomass and graphite was 10.8 ± 1.5‰ ($n = 23$), and between *Methanobacterium thermoautotrophicum* Δh cell biomass and graphite was 14.3 ± 7.5‰ ($n = 3$). The magnitude and direction of the matrix effect observed, which makes cell biomass appear more depleted in $^{13}$C than graphite, is in good agreement with previous studies [13, 14].
9. Sediment cores from Eel River Basin methane seeps were processed shipboard and sectioned into 1-cm rounds. Samples were diluted 1:1 with filter sterilized phosphate-buffered saline (PBS) (30 mM $NaPO_4$ and 390 mM NaCl) and fixed overnight with 4% formaldehyde. Samples were then washed twice with PBS and stored in PBS/ethyl alcohol (1:1) at −20°C. Sediment samples were diluted (1:5) in PBS to 1 ml final volume and treated with 20 s of mild sonication at 30 amps (Sonics and Materials Inc., Danbury, CT). Aggregates were then separated from the diluted sediment matrix and concentrated by using a fixed Percoll gradient (Sigma). Gradients were established before adding the sample by diluting the Percoll 1:1 with PBS (10 ml final volume) and centrifuging for 30 min at 38,000g. Sample (500 μl) was overlaid on the Percoll gradient and centrifuged again at 4°C for 15 min at 4400g. Separated aggregates were concentrated on a 2-μm polycarbonate filter, washed twice with 2 ml PBS, and then transferred from the filter to an untreated 1″ round glass slide. Cell transfers were conducted by spotting 5 μl of PBS onto the round glass slide and placing the filter upside down on the slide until dried. Before hybridization, slides were dehydrated in series consisting of 2-min incubations at 50%, 75%, and 100% ethanol ($n = 4$).
10. Microbial biomarkers were analyzed according to protocols reported earlier [24].
11. $\delta^{13}$C = [($R_{sample}$ − $R_{PDB}$)/$R_{PDB}$] × 1000, where PDB refers to the carbon isotopic standard with $^{13}$C/$^{12}$C = 0.011237.
12. Typical analytical precision for the SIMS analyses was about ±1‰ (1σ) within each depth profile

and better than ±3.3‰ (1σ) between different ion microprobe targets. Each analysis is the weighted mean of a set of cycles (usually 15 cycles) ± the standard error on the mean for the set of cycles. This calculated precision is appropriate for the comparison of analyses made during the depth profiling of a single spot, but it does not account for spot-to-spot reproducibility between different cell aggregates, which was determined to be better than ±3.3‰ (1 SD) based on the reproducibility of the graphite powder analyses. Analyses were required to have count rates of greater than 500,000 counts per second on $^{12}C$ because of the background of the Faraday cup detector.

13. C. H. House et al., Geology **28**, 707 (2000).
14. K. D. McKeegan, R. M. Walker, E. Zinner, Geochim. Cosmochim. Acta **49**, 1971 (1985).
15. S. J. Mojzsis et al., Nature **384**, 55 (1996).
16. C. Paull, personal communication (2001). The mean δ$^{13}$C value of methane is −50.4‰ (n = 28).
17. V. Brüchert, L. M. Pratt, T. F. Anderson, S. R. Hoffmann, in Proceedings of the Ocean Drilling Program, Scientific Research, J. P. Kennett, J. Baldauf, M. Lyle, Eds. (Ocean Drilling Program, College Station, TX, 1995), pp. 219–229.
18. Archaeol and sn-2-hydroxyarchaeol were present in the oil seep sample in quantities too low for determination of their isotopic composition, but a careful examination of the m/z 45/44 ratio trace indicated relatively high δ-values for both components.
19. Some of the variation in these analyses may be attributed to analytical difficulties resulting from the probing of single cells from culture, not encountered during the analysis of cell aggregates. However, the variation observed is substantially greater than the reproducibility found during the repeated analysis of the graphite powder standard, reflecting some degree of organism-specific heterogeneity, probably magnified by culture conditions. The similarity of these mean carbon isotopic compositions to the bulk δ$^{13}$C values of each cell culture (−17.8 and −23.6‰, respectively) demonstrates the accuracy of our reported ion microprobe analyses once matrix effects are appropriately corrected.
20. The δ$^{13}$C ion microprobe analysis is an average carbon isotopic composition for all carbon exposed to the sputtering process. However, typically organic carbon has a sputter ionization yield about 100 times that of carbonate carbon.
21. R. E. Summons, P. D. Franzmann, P. D. Nichols, Org. Geochem. **28**, 465 (1998).
22. T. M. Hoehler, M. J. Alperin, D. B. Albert, C. S. Martens, Glob. Biogeochem. Cycles **8**, 451 (1994).
23. D. L. Valentine, W. S. Reeburgh, Environ. Microbiol. **2**, 477 (2000).
24. K.-U. Hinrichs, R. E. Summons, V. J. Orphan, S. P. Sylva, J. M. Hayes, Org. Geochem. **31**, 1685 (2000).
25. K.-U. Hinrichs, A. Boetius, in Ocean Margin Systems, G. W. Wefer et al., Eds. (Springer-Verlag, Heidelberg, in press).
26. M. Elvert, E. Suess, J. Greinert, M. J. Whiticar, Org. Geochem. **31**, 1175 (2000).

# Persistence of Native-Like Topology in a Denatured Protein in 8 M Urea

## David Shortle* and Michael S. Ackerman

Experimental methods have demonstrated that when a protein unfolds, not all of its structure is lost. Here we report measurement of residual dipolar couplings in denatured forms of the small protein staphylococcal nuclease oriented in strained polyacrylamide gels. A highly significant correlation among the dipolar couplings for individual residues suggests that a native-like spatial positioning and orientation of chain segments (topology) persists to concentrations of at least 8 molar urea. These data demonstrate that long-range ordering can occur well before a folding protein attains a compact conformation, a conclusion not anticipated by any of the standard models of protein folding.

In recent years, attention has turned to structural characterization of proteins whose native state has broken down in a major conformational transition termed unfolding or denaturation. When nuclear magnetic resonance (NMR) data for several small proteins (1, 2) is combined with hydrodynamic and small-angle x-ray scattering data, the picture emerges that protein chains are relatively compact under mildly denaturing conditions, forming intermediates sometimes referred to as molten globules. As conditions are made less favorable for structure formation, most commonly by adding the chemical denaturants urea or guanidine hydrochloride, the denatured state gradually loses its residual structure and increases in size (3). At the highest concentrations of denaturants, the ensemble of conformations is expected to converge toward those of a statistical random coil.

One protein whose denatured states have been extensively studied is staphylococcal nuclease, a small α+β protein of 149 amino acids that lacks disulfide bonds or structural cofactors. Its relatively low stability allows the folded state to be broken down by a variety of perturbations. In the presence of 5 M urea, small-angle x-ray scattering has shown that the chain expands to a radius of gyration of almost 35 Å, more than twice the native state value of 16 Å (4). Nuclease can also be denatured by removing a few amino acid residues from both ends of the chain. The Δ131Δ fragment system, consisting of residues 10 to 140, refolds only in the presence of tight-binding ligands (5). In buffer at 32°C, it forms a somewhat expanded denatured state, with a radius of gyration approximately 1.3 to 1.5 times that of the folded

state. A de novo structure determination of Δ131Δ using paramagnetic relaxation from 14 extrinsic spin labels revealed that many features of the folded arrangement of segment positions and orientations persist in this model denatured state (6). Application of this same method to a less structured form of nuclease, the low-salt, acid-denatured form, failed because the measured distance restraints were insufficient to constrain the ensemble of allowed conformations (7).

An alternate NMR approach to structure determination involves imposing a slight orientation on a macromolecule in solution by forcing it to tumble in an asymmetric environment (8). The small resulting alignment leads to incomplete cancellation of the dipolar coupling between magnetic nuclei close in space. The residual dipolar coupling $D_{AB}$ contains information on the relative orientation of the vector between nuclei A and B with respect to one unique molecular axis determined by the molecular alignment tensor. Alternatively, the information can be interpreted in terms of angular relations between pairs of bond vectors that are independent of the intervening distance (9, 10). With information from residual dipolar couplings alone, relatively high-resolution structures of the backbone can be calculated (11). Although physical theory suggests there would be complexities in converting dipolar couplings measured in a denatured protein into sets of orientational restraints (12), this approach is especially attractive because the structural information is distance independent.

To orient the denatured fragment Δ131Δ of staphylococcal nuclease, we used strained polyacrylamide gels (13, 14). After diffusing a concentrated solution of protein into a gel cylinder and sliding it to the bottom of an NMR tube, the gel cavities were distorted from their initial spherical symmetry to ellipsoidal symmetries by mechanical compression (15). Given the chemical inertness of polyacrylamide, it is assumed that proteins interact with the gel matrix only through

Department of Biological Chemistry, The Johns Hopkins University School of Medicine, Baltimore, MD 21205, USA.

*To whom correspondence should be addressed. E-mail: shortle@welchlink.welch.jhu.edu